KERNFORSCHUNGSZENTRUM

KARLSRUHE

Oktober 1968

KFK 874
EUR 4157 e

Institut für Reaktorentwicklung

Liquid Metal Boiling Research

W. Peppler, G.F. Schultheiss

GESELLSCHAFT FÜR KERNFORSCHUNG M.B.H.

KARLSRUHE

KERNFORSCHUNGSZENTRUM KARLSRUHE

Oktober 1968

KFK 874

EUR 4157 e

Institut für Reaktorentwicklung

Liquid Metal Boiling Research *)

W.Peppler

G.F.Schultheiss

Gesellschaft für Kernforschung mbH.,Karlsruhe

---

*) Work performed within the association in the field of fast reactors between the European Atomic Energy Community and Gesellschaft für Kernforschung mbH.,Karlsruhe.

Liquid Metal Boiling Research

W.Peppler
G.F.Schultheiß

Institut für Reaktorentwicklung
Kernforschungszentrum Karlsruhe

Introduction

Interest and research in boiling processes generally and liquid metal boiling in particular have been enhanced by power reactor development and safety considerations. Therefore, an extensive research program has been established for experimental investigations of boiling phenomena and background information for various liquids and in particular for liquid metals.

The Karlsruhe program on this special subject has been described in more detail in [1]. The experimental work is related to theoretical investigations with special emphasis being placed on sodium-cooled fast reactor safety aspects. Under certain circumstances, a positive coolant void coefficient in connection with sodium boiling may lead to a destructive accident. As described in [1] the coolant behaviour during boiling depends on liquid metal superheat as well as ejection and re-entry mechanisms within a fuel assembly.

In order to predict the sequence of events during boiling in sodium-cooled reactors two lines are pursued to obtain experimental results. In one line, all experiments are performed with water or organic coolants to permit the use also of optical observation and high-frequency movie. Under specific conditions results obtained from these experiments can be compared or even extrapolated to those carried out with liquid metals. Those liquid metal experiments constitute the other line, which can be employed to gain more insight into boiling processes.

First results of sodium-experiments on incipient boiling superheat and liquid expulsion are reported in the following two papers already presented at the Liquid Metal Boiling Meeting at Ispra, October 10 - 11, 1968.

INFLUENCE OF CAVITIES AND OXIDE CONCENTRATION ON SODIUM SUPERHEAT *

G.F.Schultheiß
Institut für Reaktorentwicklung / Kernforschungszentrum Karlsruhe

The superheat required for incipient boiling of liquid sodium is of considerable influence in the safety analysis of sodium-cooled fast reactors. Sodium superheat values in boiling processes are about ten times higher than those of water for the same critical bubble radius, especially as a result of higher boiling point and surface tension and lower vapor density as can be seen from the Laplace equation (1) [2] and the Clausius Clapeyron-equation (2)

$$p_v + p_g - p_l = \frac{2\sigma}{r^*} \tag{1}$$

$$\frac{dp}{dT} = \frac{\Delta h\, \rho_l\, \rho_v}{T(\rho_l - \rho_v)} \approx \frac{\Delta h\, p}{RT^2} \tag{2}$$

from which it follows by integration and approximation of the logarithm factor for low superheat values

$$T_v - T_s = \frac{2\sigma\, T_s}{\Delta h\, \rho_v\, r^*} \tag{3}$$

with

Δh	heat of vaporization
p	pressure
R	gas constant
r^*	critical radius of nucleus
ρ	density
σ	surface tension
T	absolute temperature

---

* Paper presented at the Liquid Metal Boiling Meeting, Ispra, October 10 - 11, 1968

subscripts

g	gas
l	liquid
s	saturation condition
v	vapor

On the other hand sodium has a high chemical aggressiveness and, therefore, thermodynamical processes which could be calculated in a rather straightforward manner will be superimposed by numerous physico-chemical reactions, depending on the state of the whole system. So, besides the conditions of heater surface roughness, also suspended and dissolved impurities may become important for the maximum possible superheat of incipient boiling.

Although a great number of experimental data are available today [3], a superheat prediction on the basis of any of the existing theories is rather difficult, because there is a very large variation of the values and often contradictory effects are reported. To obtain some more insight into liquid sodium boiling behaviour, an experimental program has been started at Karlsruhe to investigate the influence of special parameters on the superheat necessary for boiling initiation. There parameters are

- geometry of artificial cavities
- sodium oxide concentration and
- amount of dissolved gas.

A flow diagram of the equipment built for this purpose is shown in Fig. 1. The experiments are performed in a test pool. A natural-convection loop with cold trap and hot trap is provided for sodium purification and test pool cleaning by rinsing. The traps are bypassed for independent use. A storage tank completes the sodium containing part of the system. The gas containing part includes the cover gas supply and purification and the vacuum pump. Two oil thermostats not shown in this diagram regulate the cold trap temperature and the temperature of a piezo quartz pressure sensor. The whole system is monitored mainly by thermocouples installed in the sodium filled part.

All data necessary for evaluation are recorded by a compensation plotter or, after amplification, by an UV-oscilloscript.

Fig. 2 shows the test pool. Except for the stainless steel bellows condenser the test chamber is arranged within an electrically heated furnace to get a uniform temperature profile in the sodium. The hot finger in the middle of the horizontal test plate at the bottom of the sodium pool is separately heated by radiation. In this figure, also the distribution of the thermocouples is demonstrated. In addition to the control of the thermodynamic state the thermocouples allow the detection of bubble nucleation and movement by temperature oscillations in the liquid phase. Therefore, the thermocouples are concentrated mainly in vertical positions in the middle of the pool above the artificial cavity. NiCr-Ni thermocouples of 0.5 mm and 1.0 mm diameter are used.

To date all experimental runs have been performed with test section No. 1 (for dimensions see Fig. 3). In the middle of a hot finger heated plate there is a cylindrical cavity of 0.4 mm diameter and 2.0 mm depth. The rest of the plate is extremly polished. The heat flux through the hot finger and the temperature at the bottom of the cavity are calculated from the output of thermocouples No. 22 and No. 23 inside the hot finger, whereas bubble nucleation and growth from the artificial cavity is detected in addition by the thermocouples No. 32 and No. 40. Boiling processes inside the test pool are also detected by an acoustical method with a magnetic phono pickup and by the piezo quartz pressure sensor.

Except for the last four ones all the experimental runs performed up to now were carried out in the absence of any cover gas and after a long period of sodium degassing. Then the system is pressurized only by the sodium vapor pressure corresponding to the thermodynamical equilibrium inside the pool and, at the bottom, additionally by the static liquid pressure. After establishment of an equilibrium inside the test pool nucleate boiling is induced by further increasing the temperature in the cavity area by means of the hot finger heating system.

Figures 4 to 7 show the first experimental results. The reproducibility of the experiments was clearly demonstrated by several series of runs. The experiments were carried out within a saturation temperature range between 500°C and 875°C. The results are plotted in diagrams calculated from (3) and show the superheat requirements for various critical bubble radii. The physical data for the calculation were taken from [4].

In Fig. 4 calculated and experimental values for hot trap purified sodium are compared. Good agreement between the cavity radius and the theoretical critical radius - both 0.2 mm - can be stated, although at higher saturation temperatures the accuracy of the measuring system leads to a higher error range. After completion of these series of runs the sodium oxide concentration was changed by purification with cold trap temperature variation. The reported concentration values are averaged from experimental solubility data [5] due to cold trap temperature (CTT).

The superheat results are plotted in Fig. 5 for oxide concentrations of

12 ppm averaged from 127°C - CTT
23 ppm averaged from 164°C - CTT and
33 ppm averaged from 185°C - CTT.

A first series of runs was carried out by stepwise increasing the oxide concentration whereas, in the repetition run, the concentration was decreased. Generally, this figure shows that superheat decreases with increasing oxide concentration. Particularly remarkable are the high values of all 12 ppm runs which are even higher than those of hot trap purified sodium. More experimental work will be necessary to prove and to explain such effects. Also other experimentally stated tendencies must be verified by further investigation with different dimensions and geometries of the artificial surface cavity.

The comparison between theoretically calculated and experimentally measured superheat values leads to the impression that the nucleation

cavity grows with increasing oxide concentration. However, since the critical nucleation radius is calculated from thermophysical properties of sodium, this comparison shows the influence of oxide concentration on these properties. Up to now, nothing is known of this influence on sodium surface tension and wetting behaviour in particular.

A special evaluation of the experiments reported was started with respect to the Holtz-Singer theory of the pressure-temperature history influence on sodium superheat necessary for incipient boiling [6, 7]. Based on specific cavity penetration assumptions this theory predicts increasing superheat values with, e.g., increasing pre-boiling system pressure. A recent report from Brookhaven [8] supports this theory.

Fig. 6 (e.g.) is a graph of a one-day sodium boiling program performed with the equipment already shown. In a first series the saturation temperature has been decreased stepwise, beginning around 800°C; this is followed by a repetition. The evaluated superheat values for incipient boiling are plotted for each saturation point and related to the repetition value. No difference is evident, which may be due to the low pressurization of only 0.4 atmospheres by sodium vapor pressure at 800°C. Hence, at the end of our present program we added a series of four experiments with gas pressurization up to 2.0 atmospheres. The sodium pool had an average oxide concentration of 12 ppm. The results are plotted in Fig. 7. Pressure and temperature as well as the superheat values of each boiling experiment are shown versus time. Again, there is no difference in superheat at boiling initiation and the values are in good agreement with the other results of the 12 ppm oxide series.

Finally, it can be said that the cavity has operated now for about six months as a nucleation center without any deactivation effect either by some long-time boiling experiments for degassing or by pressure temperature variation. Due to this very surprising fact - surprising, since we also believed in extreme deactivation tendencies of liquid sodium - no corroboration of the investigated theory [6, 7] can be given.

On the other hand, the dimensions of the cavity are of the same order of magnitude as those of the gaps between fuel pins and spacers in reactor subassemblies; therefore, these results caused the construction of an experiment for the investigation of the influence of spacers on sodium superheat for incipient boiling on a fuel pin-type heater rod. From the results shown here it is possible to anticipate very stable nucleation centers and low superheat values at normal boiling point or higher system pressure with all consequences for the safety analysis.

BOILING EXPERIMENTS IN A LARGE SODIUM LOOP USING INDUCTION HEATING *

W. Peppler
Institut für Reaktorentwicklung / Kernforschungszentrum Karlsruhe

1. Introduction

To recognize the process of liquid metal boiling and recondensation phenomena and to back up and improve analytical models an extended experimental research program is being executed. The program was outlined by Karlsruhe and Ispra. Today, the first 45 tests in the Karlsruhe sodium boiling loop (NSK) have roughly been evaluated; they contribute to an answer to these basic three questions:

1) What degree of liquid superheat will be reached before boiling starts?

2) How fast will the channel be voided and how fast does the void diminish again by re-entrant sodium?

3) What destructive mechanism may result during re-entry or recondensation of sodium into the voided channel?

2. Test Facility

Before the results are discussed, a short survey of the test installations will be presented. The first figure (Fig. 8) shows the sodium loop with the containment open. During the tests it is closed and filled with nitrogen to prevent fires.

The scheme of the sodium loop with the test section is shown in Fig. 9. The loop consists of EM pump, control valve, preheater, test section, expansion tank, and recooler. The test section is made of a stainless steel tube 1 m long with an outside diameter of 15 mm and a wall

---

* Paper presented at the Liquid Metal Boiling Meeting, Ispra, October 10 - 11, 1968

thickness of 1.5 mm. It is indirectly heated over a length of 500 mm by the HF heating device developed at Karlsruhe. A maximum heat flux of 700 W/cm^2 with respect to the inner wall of the tube has been reached. This is more than 3 times the maximum design value at the surface of the fuel pins of the sodium fast breeder (215 W/cm^2). A further increase in heat flux is possible. Since the method is restricted to tube geometries, other indirect heating devices have been discussed and investigated. They all lacked the ruggedness necessary to survive the severe shocks of a large number of expulsion experiments.

During the tests all data such as temperature, pressure, flow, and power, which are important for the dynamic behaviour were recorded on a 24-channel-visicorder.

The design of the loop makes it possible to simulate the following failure conditions with respect to the reactor:

- Total and sudden blockage of one fuel channel. (The fast operating control valve is closed, the heat input to the test section remains unchanged.)
- Loss of pumping power (the EM pump is turned off).
- Partial blockage of one fuel channel (the flow is reduced in the test section by throttling with the control valve).

3. Results

In this test loop 45 expulsion runs were made within a static boiling pressure range of 0.5 to 1.3 ata.

The results of the runs are:

1) Superheat

- The superheat values measured differ by more than one decade. This is true also of immediately following runs in which all

controllable parameters, i.e. heat flux, temperature, pressure, flow, and impurity content, are kept constant. In Table 10 all results are summarized in groups. The first and the second group show nearly the same level. Beyond 60°C it falls off rapidly.

- The average of all superheat values grows with increasing number of test (Diagram 11). This points to the well known fact that after repeated boiling part of the nucleation sites become inactive.

- A dependency of the superheat on the boiling temperature cannot be observed from the experiments (Diagram 12), although theoretical calculations and a large number of other experiments predict an increasing superheat with decreasing temperature.

- The location of highest superheat at the wall of the test section must not be the place where the void starts.

- The averaged superheat values for tests No. 16 to 45 increase with increasing heat flux as can be seen from Diagram 13. Because of the starting effects already mentioned it was decided not to include tests No. 1 to 16. This tendency must still be proven by more tests.

2) Expulsion

Some tests were considered in more detail for better understanding of the mechanism of the first expulsion. In Diagram 14 the measured void velocity vs the time from the beginning of the expulsion was included as well as the integrated curve. With these time-dependant values, which are the velocity and void and the acceleration seen in Diagram 15, together with the measured hydraulic resistance characteristic of the test section the driving pressure difference could be determined. A piston type model was assumed for the expulsion mechanism. Since the magnitude of the driving pressure difference is related to the measured superheat, all values are transferred to

superheat values. This so-called "driving superheat" is shown in the diagram. For experiment No. 4 the measured superheat at the wall at the beginning of the first expulsion was 28°C, in the center of the channel it was 16°C. As it was not always possible to locate the exact place where the void started, the middle of the heated section and the middle of the upper third were assumed. This results in the upper and lower curves for the driving superheat. It is seen that at the beginning of the expulsion the measured superheat is higher than the driving superheat. This is true of all tests evaluated. During the expulsion the driving superheat approaches the measured value.

At the end of the more detailed consideration, test No. 34 (Diagrams 16 and 17) is shown. The course is more violent than in the former test. Thus, the driving superheat within 110 msec increases from 12°C to the maximum of 67°C, which corresponds quite well to the measured superheat of 74°C.

When the extension of the void is compared at the moment the steep decrease of the acceleration begins, it is seen that it has just reached the upper unheated part of the test section. So, the fast condensation of vapor on the cold walls must be responsible for the steep decrease.

In general, the evaluation of these tests allows the following conclusions:

- At the beginning of the expulsion the measured wall superheat and even the superheat in the center of the channel are 2 - 4 times higher than the driving superheat.

- With growing void the driving superheat approaches the measured superheat up to 90 %.

- As soon as the void has reached the unheated section, the acceleration decreases very fast. The violent condensation process in the unheated part of the test section overrides the evaporation in the heated section, even for a heat flux of 220 W/cm^2.

- In all tests independent of heat flux, a repeated expulsion and re-entry of sodium was observed. The pulsations proved to be a very efficient cooling of the test section. The maximum wall temperature did not exceed 1150°C even after several expulsions and re-entries under load. This may mean that for some while the fuel pins in a reactor can withstand a total blockage of a channel without melting.

- The average of the total void during the first expulsion increases with increasing heat flux. This tendency is caused not so much by the higher heat flux but by the higher superheat, as shown before.

- The first expulsion is the most violent one only in 20 % of all tests.

  The first consecutive 1 - 3 expulsions of one run show that in nearly all cases the void develops in the upper heated part of the test section while the sodium in the lower part does not move. This leads to a higher superheat in this part followed by a vigorous expulsion. Often, it could be observed that the column of sodium accelerated by the vaporisation (void) in the lower part of the test section collides with the liquid reflux sodium thrown out earlier by the vaporisation (void) in the upper part. This type of behavior has some similarity to slug flow.

3) Re-entry of Sodium and Recondensation Pressure Pulses

Finally, some results of the re-entry mechanism of sodium and the recondensation pressure pulses are compiled:

- The averaged values of the pulsation frequency grow with increasing heat flux (Diagram 18).

- Under heat load conditions during the re-entry of sodium a certain quantity of vapor always remains.

- The pressure peaks at the end of the re-entry of sodium extend as high as 30 atm (Table 19). The duration of the pulses is less than 1 msec. The structure of the test section was not affected by them. Sometimes, the peaks are higher at the end of a re-entry under heat load conditions, sometimes the final re-entry, the so-called recondensation, shows the highest peaks.

A more detailed evaluation of the expulsion mechanism with the calculation code "Blow" is on the way [9]. The results of that work will be reported later on.

References:

[1] Smidt,D., Fette,P., Peppler,W., Schlechtendahl,E.G., Schultheiss,G.F., Problems of Sodium Boiling in Fast Reactors, KFK 790, EUR 3960e, June 1968

[2] Laplace,P.S., Mecanique Celeste, Supplement, Vol. 10, 1806, as quoted by Defay,R., et.al. in Surface Tension and Adsorption, Longmans, London, 1966, p. 7

[3] Fauske,H.K., Superheating of Liquid Metals in Relation to Fast Reactor Safety, Reactor Fuel Processing and Technology, Vol. 11, No. 2, 1968, pp. 84-88

[4] Golden,G.H., Tokar,J.V., Thermophysical Properties of Sodium, ANL 7323, August 1967

[5] Claxton,K.T., Contribution on the Solubility of Oxygen in Liquid Sodium, J.Nuclear Energy 1967, Vol. 21, pp. 351-357

[6] Holtz,R.E., The Effect of the Pressure-Temperature History upon Incipient-Boiling Superheats in Liquid Metals, ANL 7184, June 1966

[7] Holtz,R.E., Singer,R.M., On the Superheating of Sodium at Low Heat Fluxes, ANL 7383, November 1967

[8] Chen,J. et.al., Heat Transfer Studies, BNL 50 089, December 1967, pp. 153-154

[9] Schlechtendahl,E.G., Die Ejektion von Natrium aus Reaktorkühlkanälen, Nukleonik 10, Heft 5, 1967.

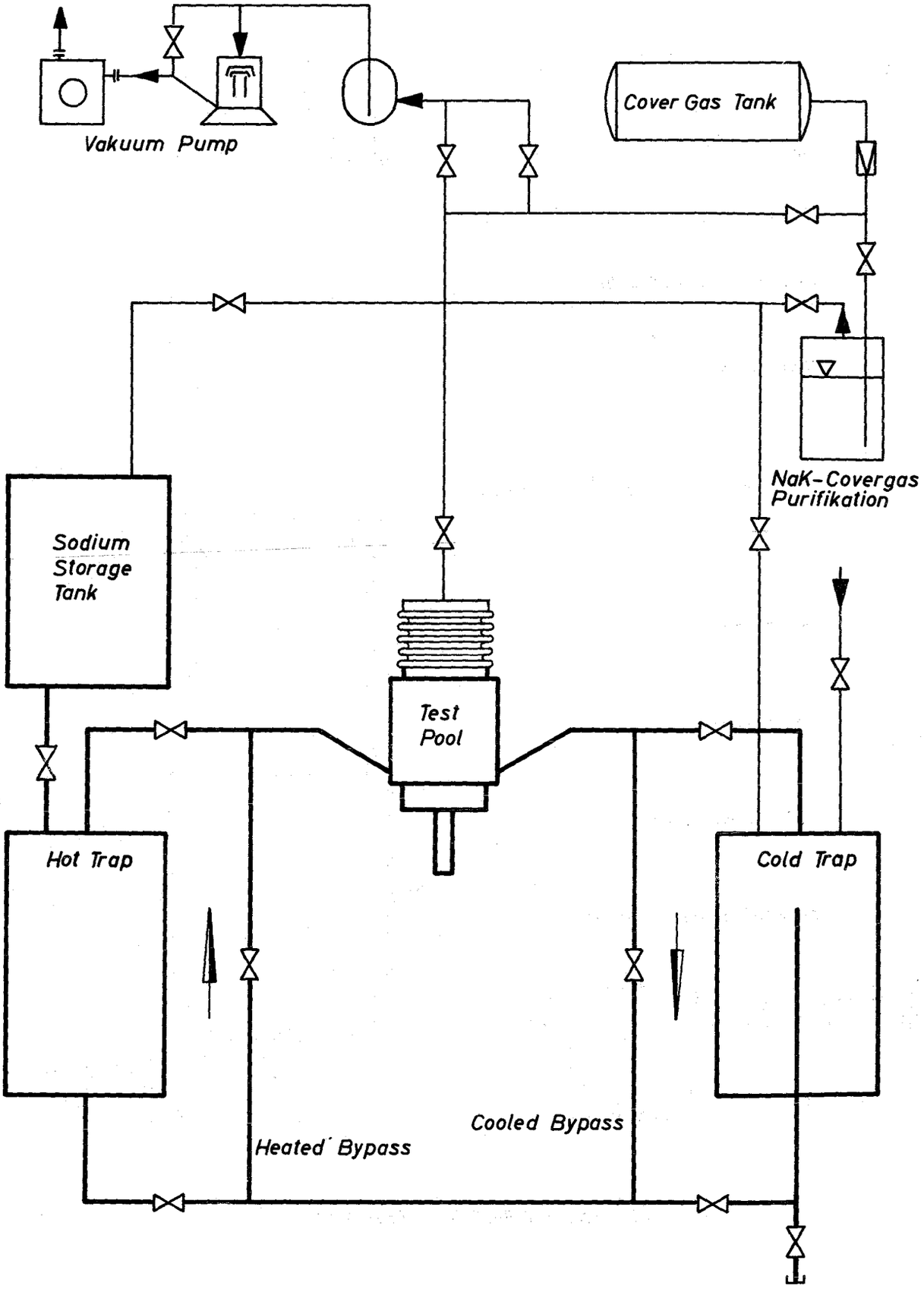

Fig. 1 FLOW DIAGRAM OF SODIUM SUPERHEAT EXPERIMENT

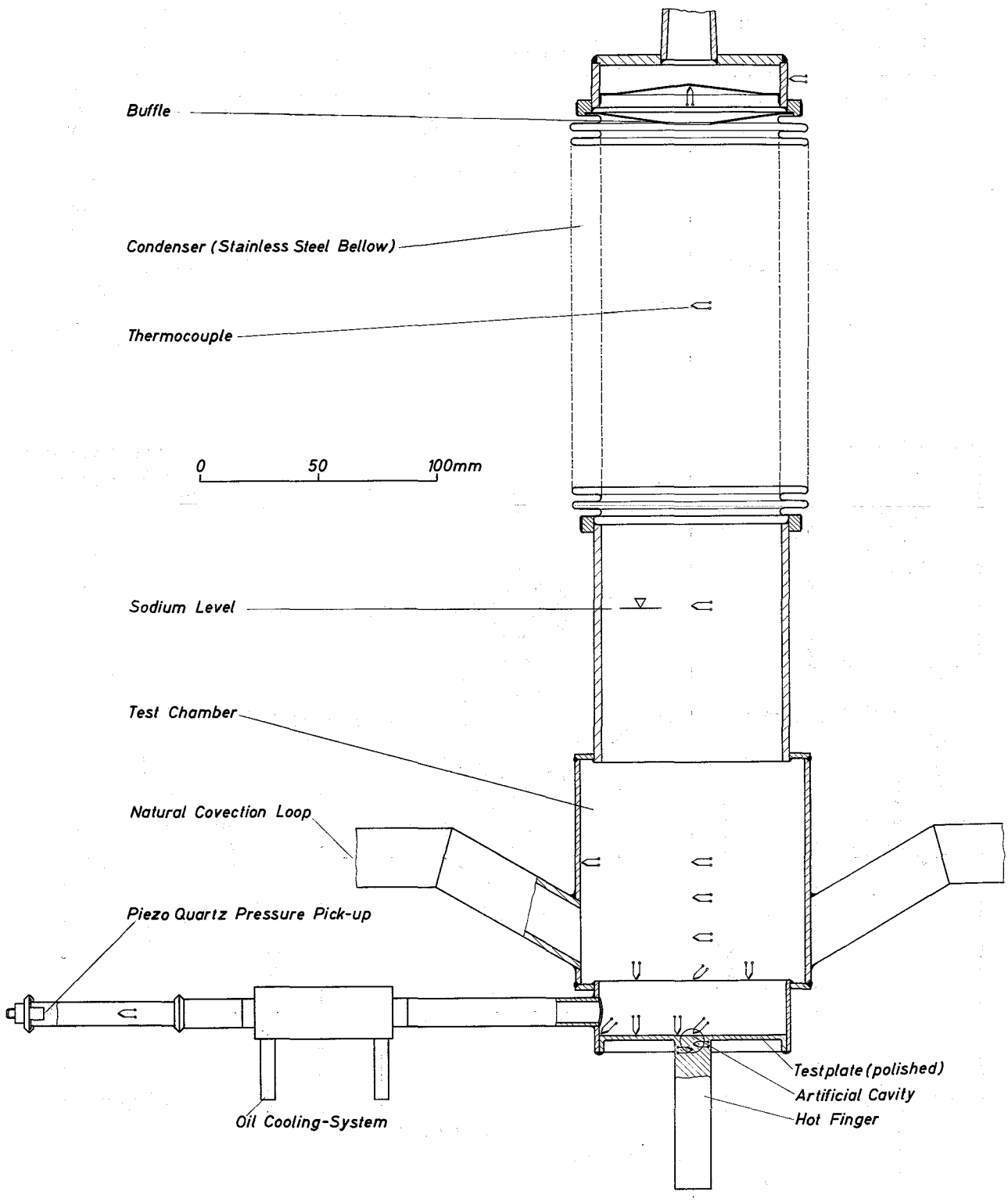

Fig.2 SODIUM SUPERHEAT TEST POOL

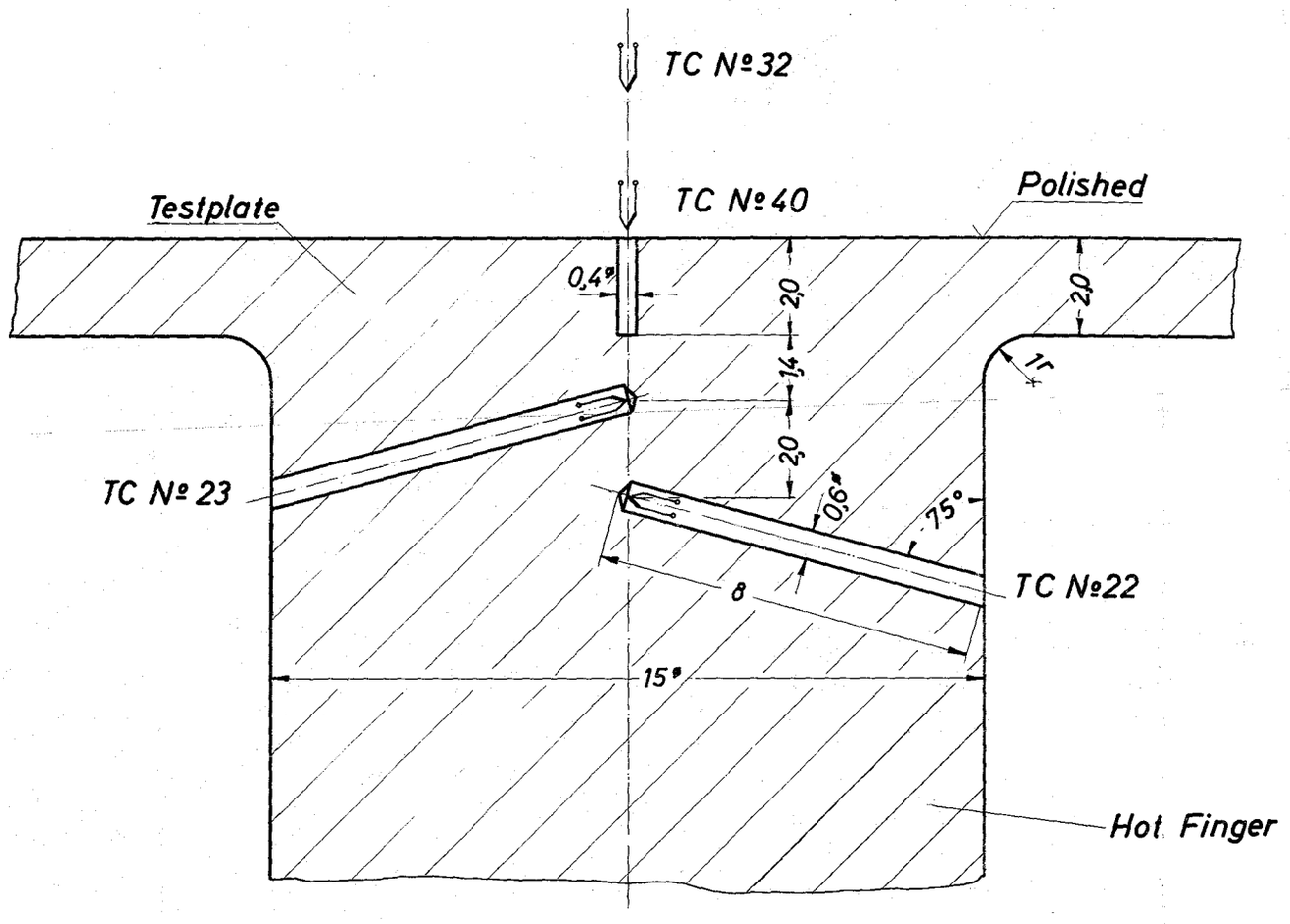

Fig.3 SODIUM SUPERHEAT EXPERIMENT
DIMENSIONS OF TESTSECTION Nº1

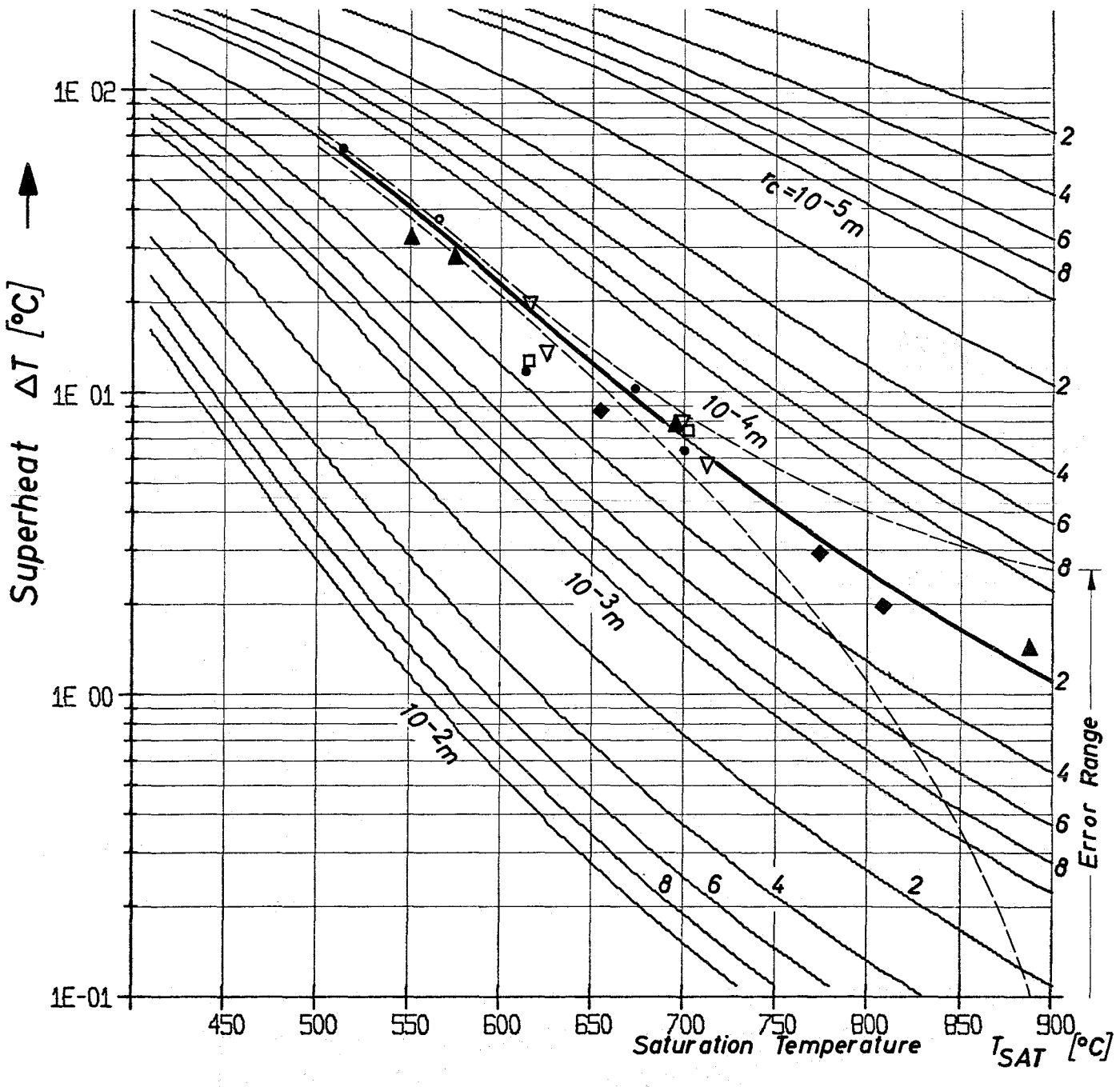

Fig. 4 HOT TRAP PURIFIED SODIUM SUPERHEAT

Busmer
8.10.68

IRE4-29-4-371

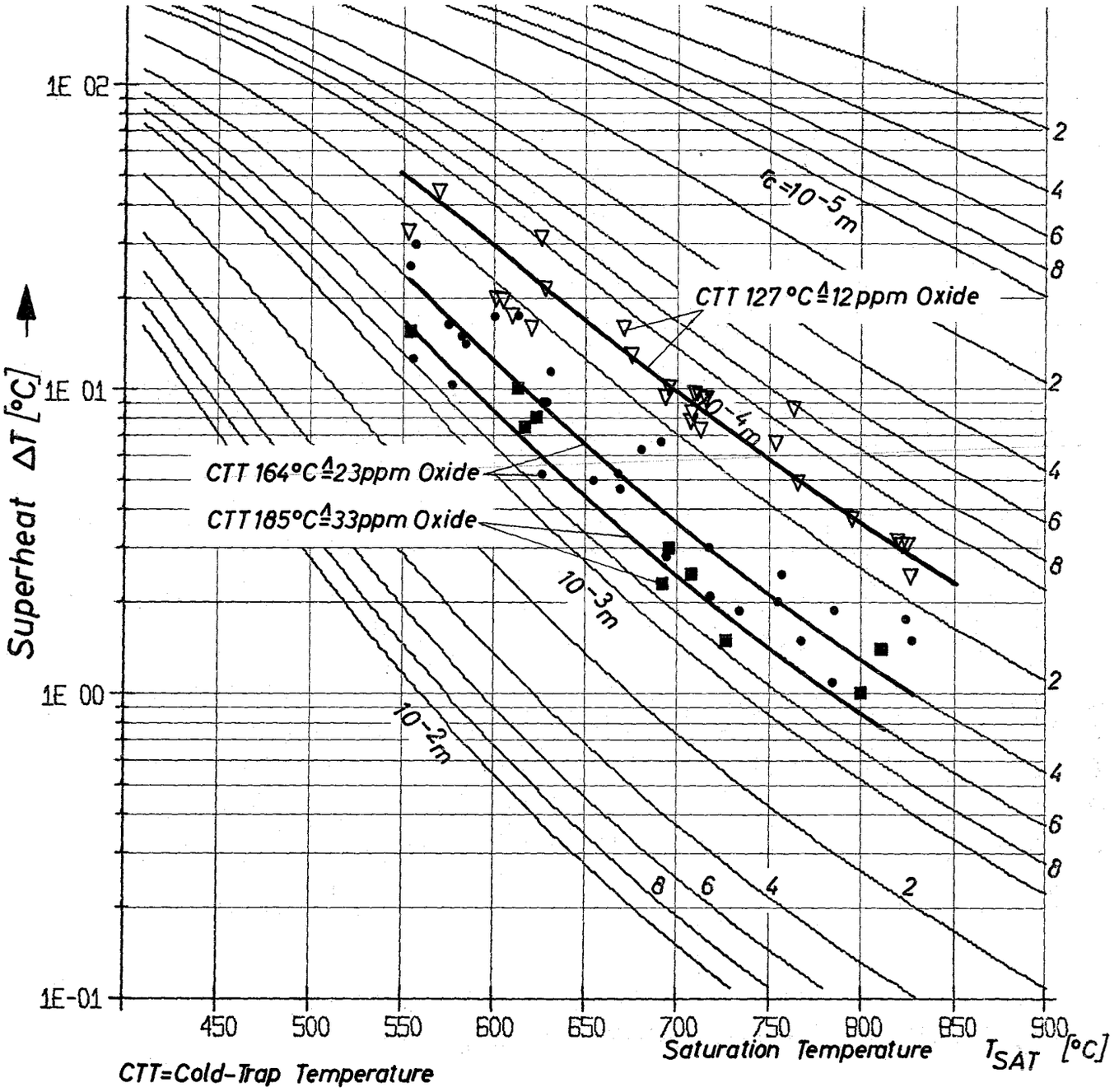

CTT=Cold-Trap Temperature

Fig. 5 INFLUENCE OF OXIDE CONCENTRATION ON SODIUM SUPERHEAT

Bussmer 8.10.68

IRE4-29-4-372

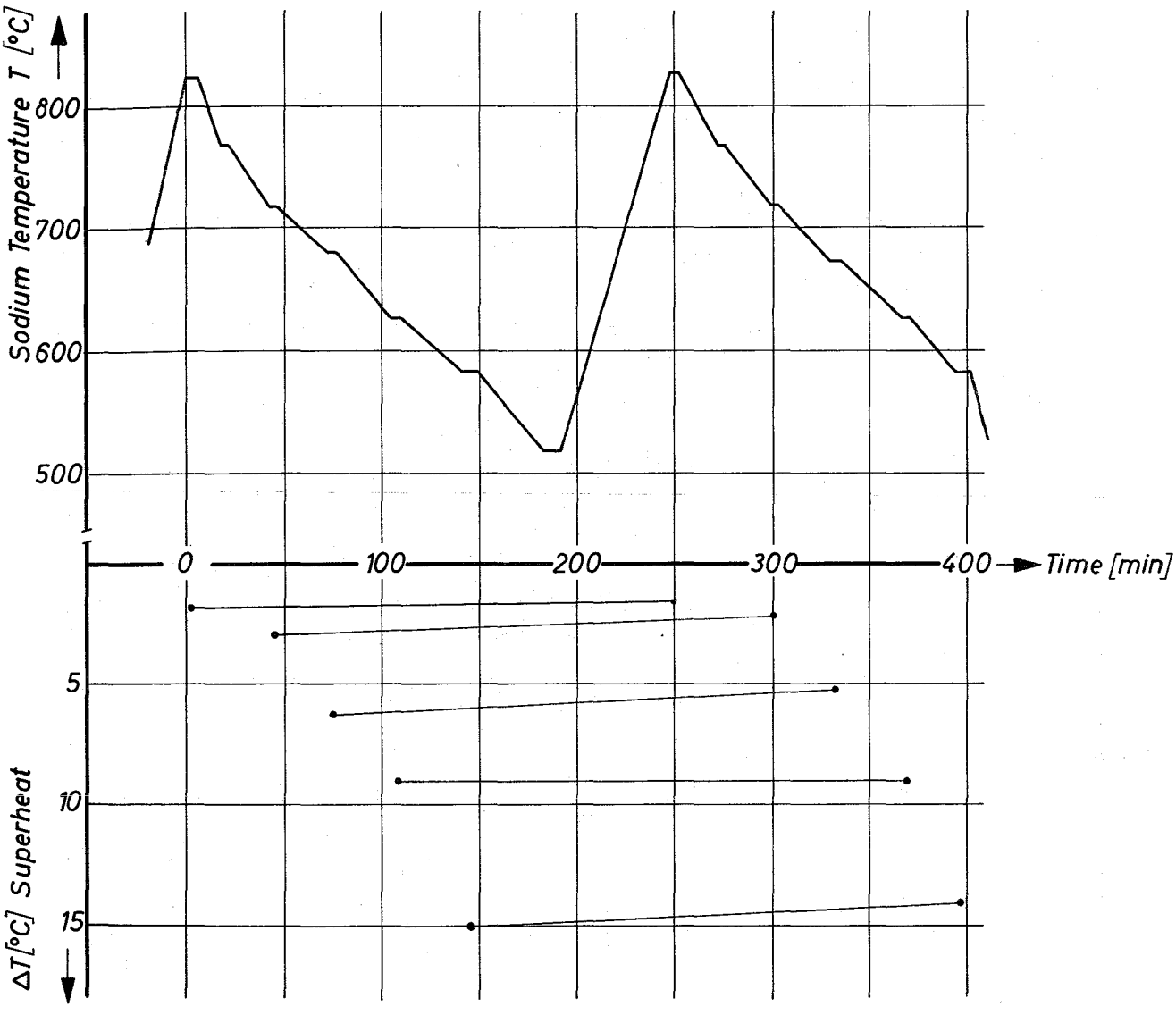

Fig.6 SODIUM BOILING SERIES OF ONE DAY

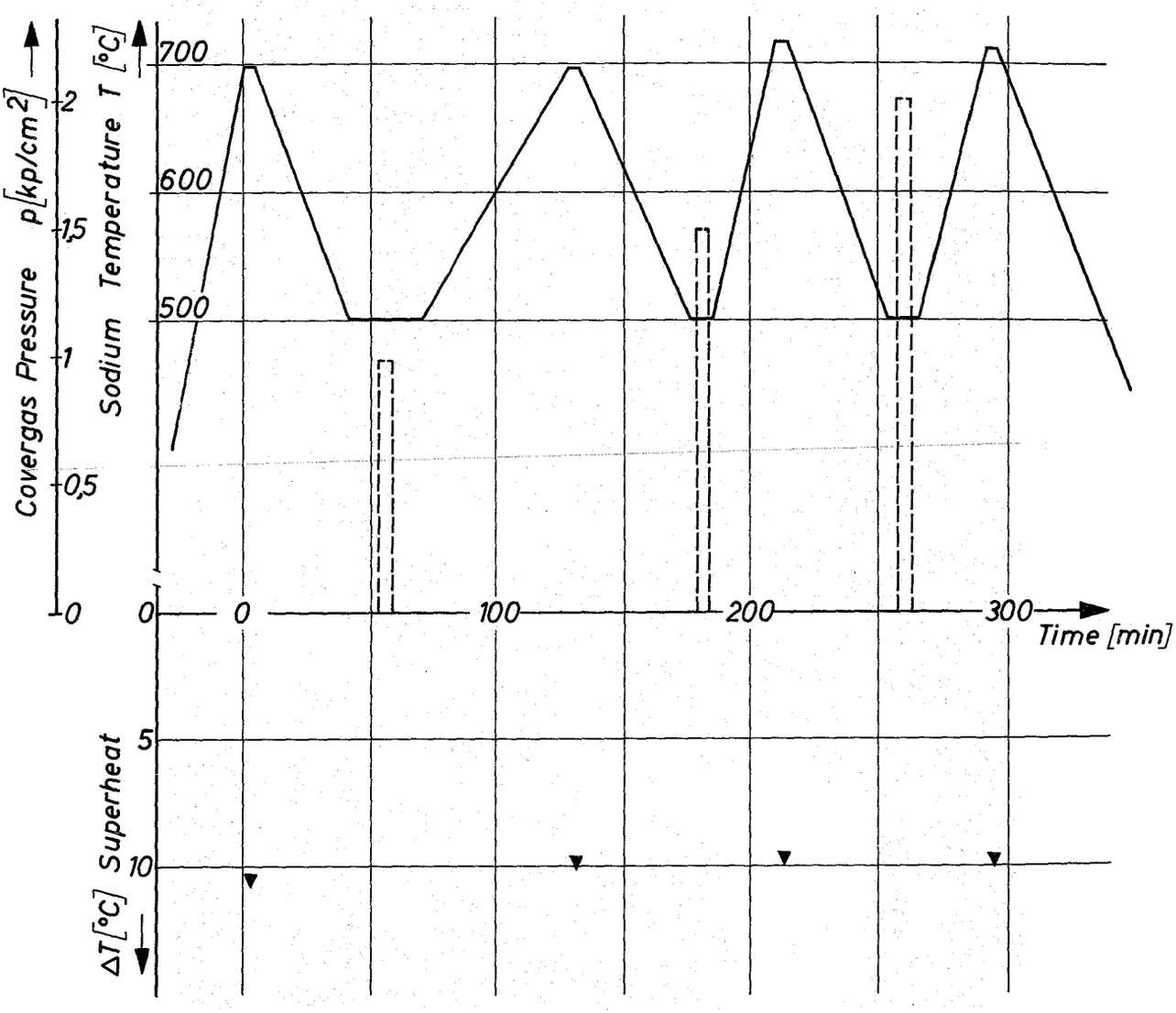

Fig. 7 SODIUM SUPERHEAT WITH PRESSURE-TEMPERATURE VARIATION

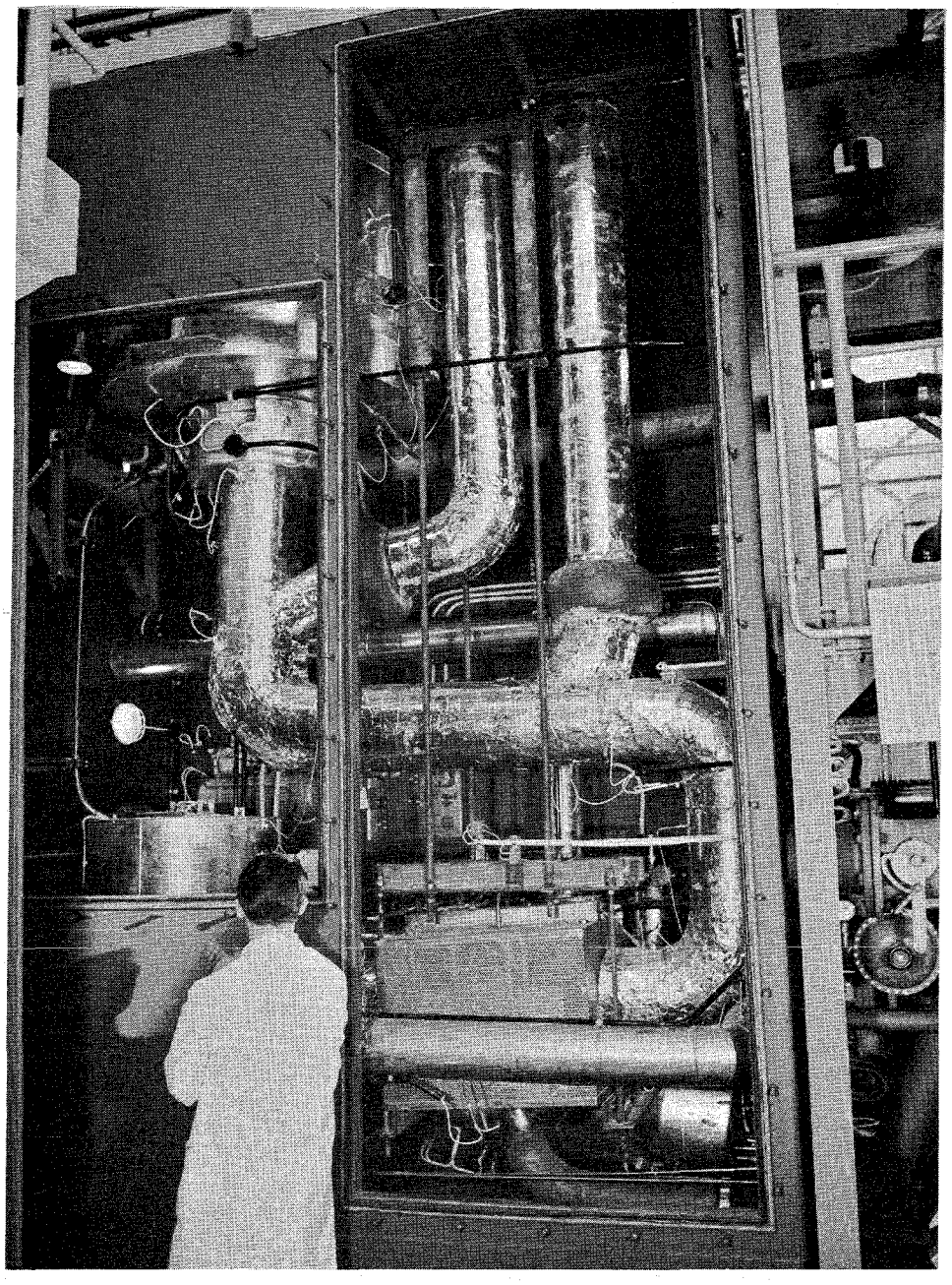

Fig.8 NSK Sodium Boiling Loop

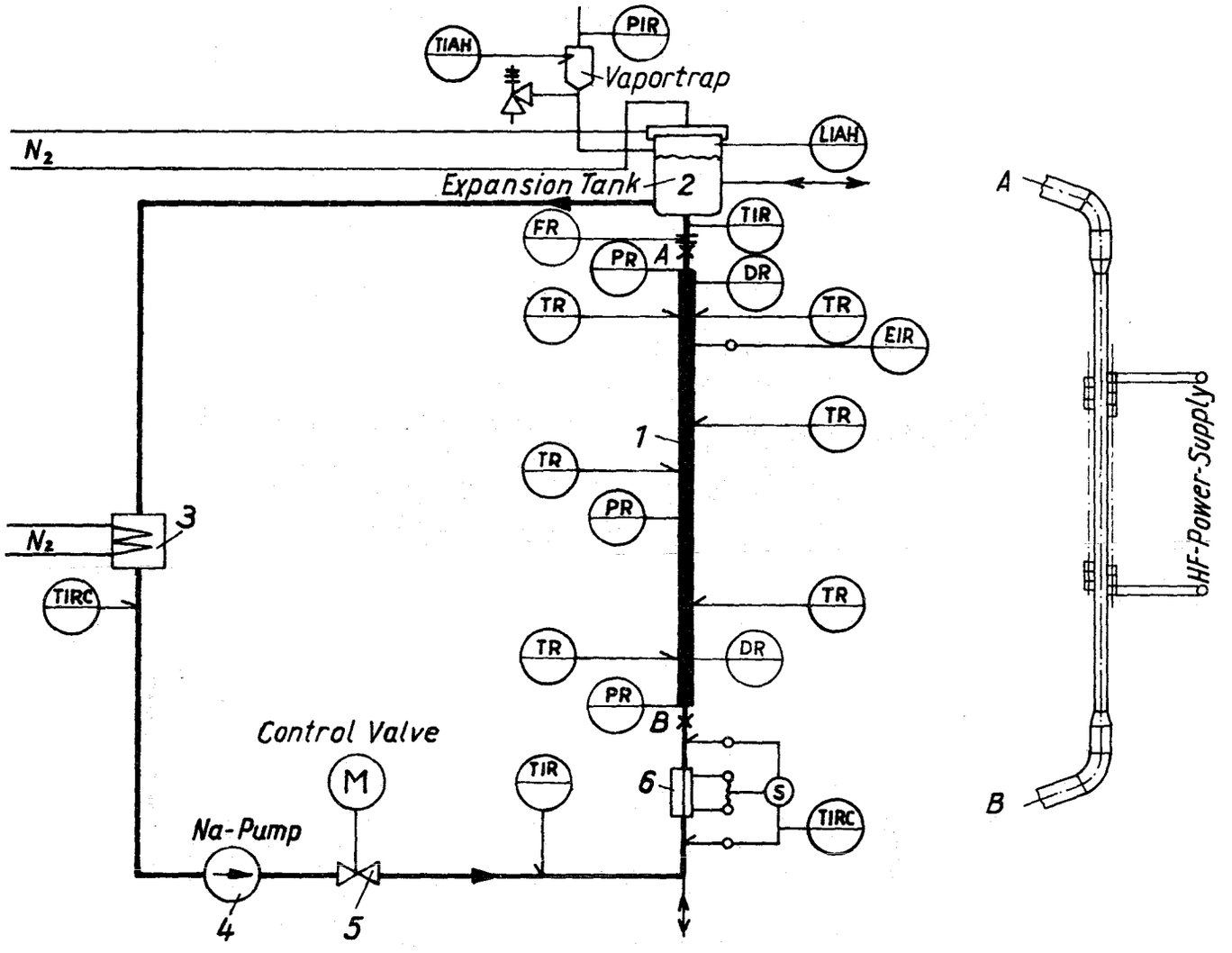

Power	E	Level	L
Temperature	T	Indication	I
Flow	F	Registration	R
Pressure	P	Alarm[High-Low]	A[HL]
Density	D	Control	C

Indication Local

Indication or Registration on Operator Desk

Fig. 9 NSK Sodium-Loop Testsection

ΔT °C	% of all tests	void in % of testsection content
20- 40	36	23,6
40- 60	33,4	29,6
60- 80	7,7	53,0
80-100	7,7	47,6
100-120	7,7	49,6
> 120	7,5	

Table10 Accumulation of Measured Superheats in the First 45 Expulsion Tests (ΔT at the Beginning of the First Expulsion) NSK

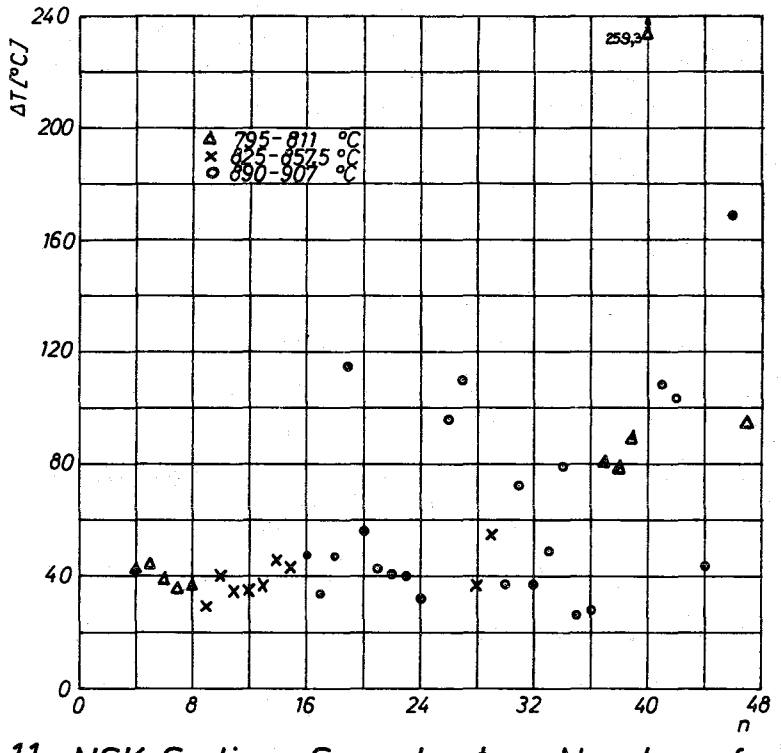

Fig.11 NSK Sodium Superheat vs Number of Experiment (Time Dependance)

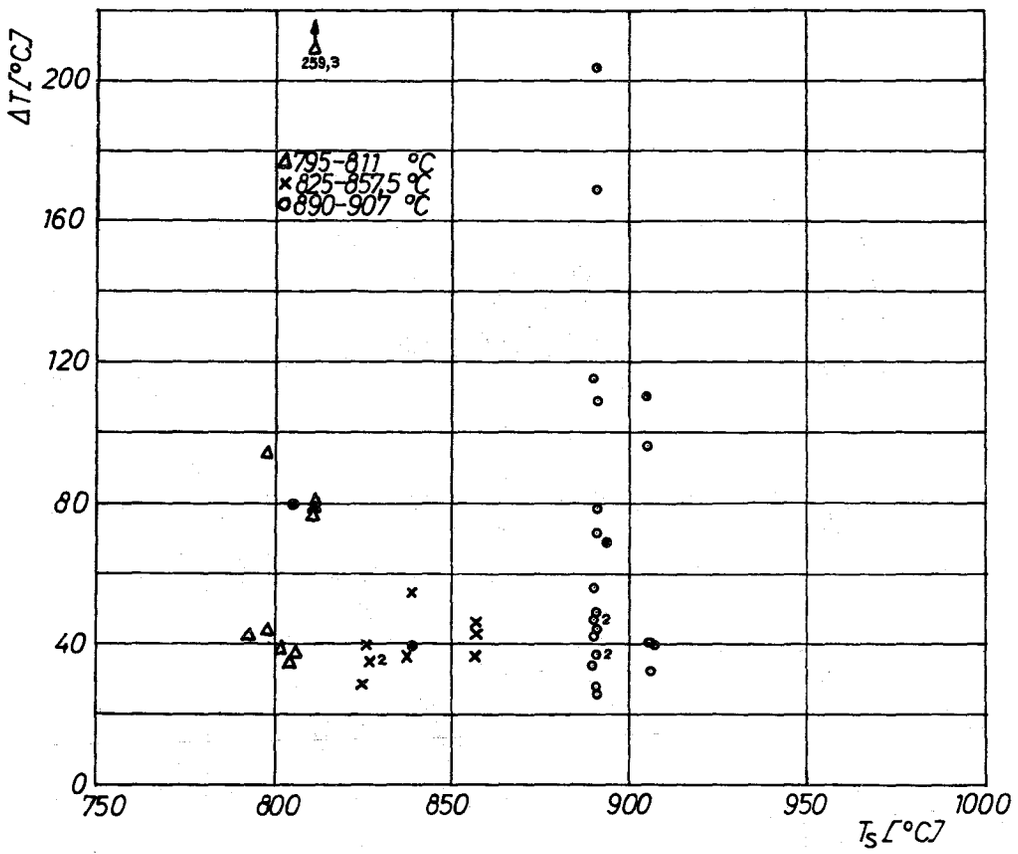

Fig.12 NSK Sodium Superheat vs Static Boiling Temperature

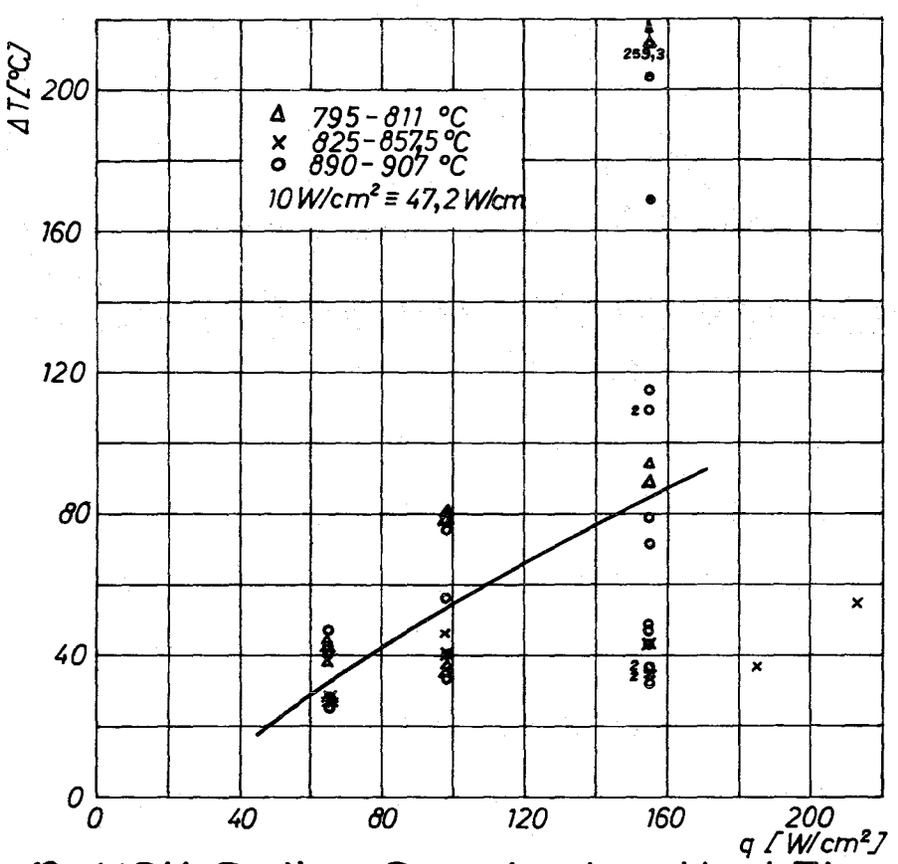

Fig.13 NSK Sodium Superheat vs Heat Flux in the Testsection

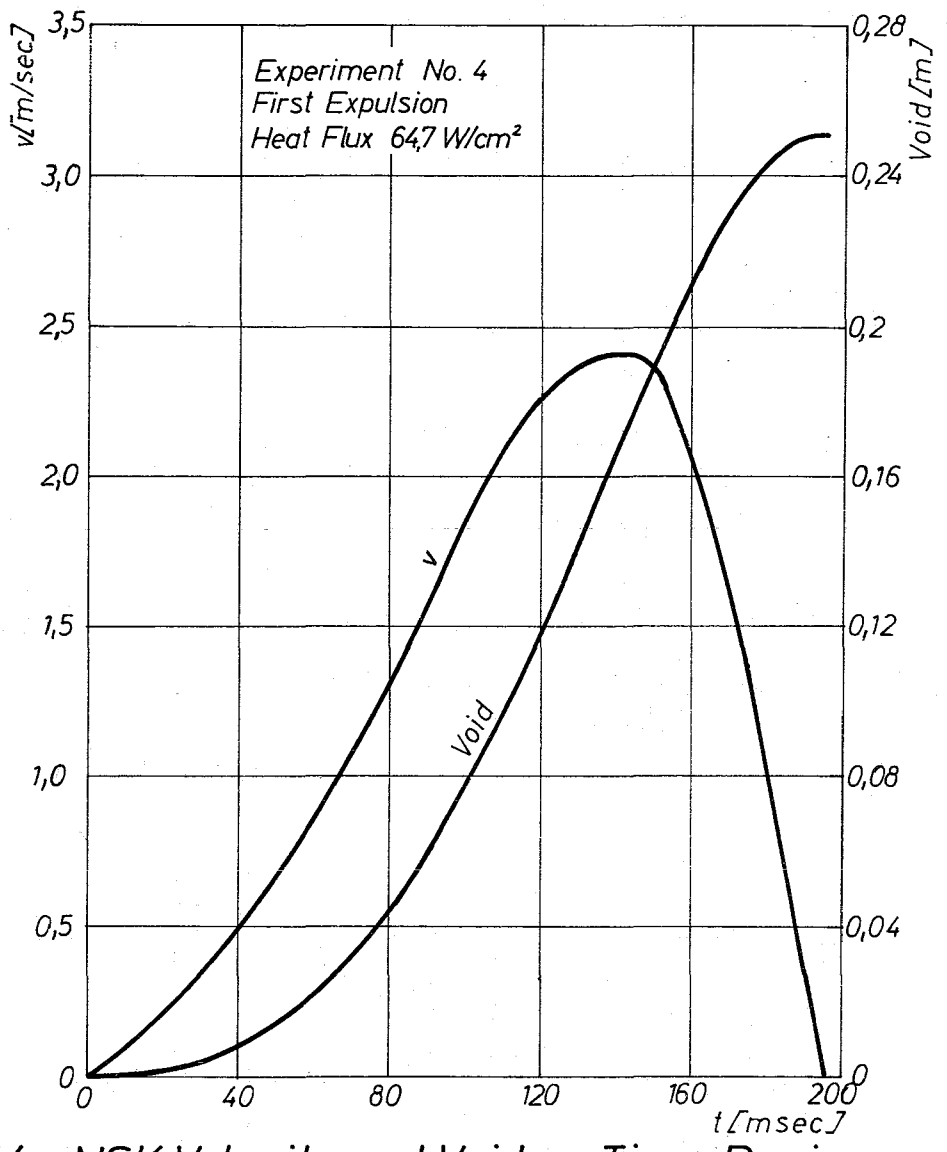

Fig. 14 NSK Velocity and Void vs Time During Expulsion

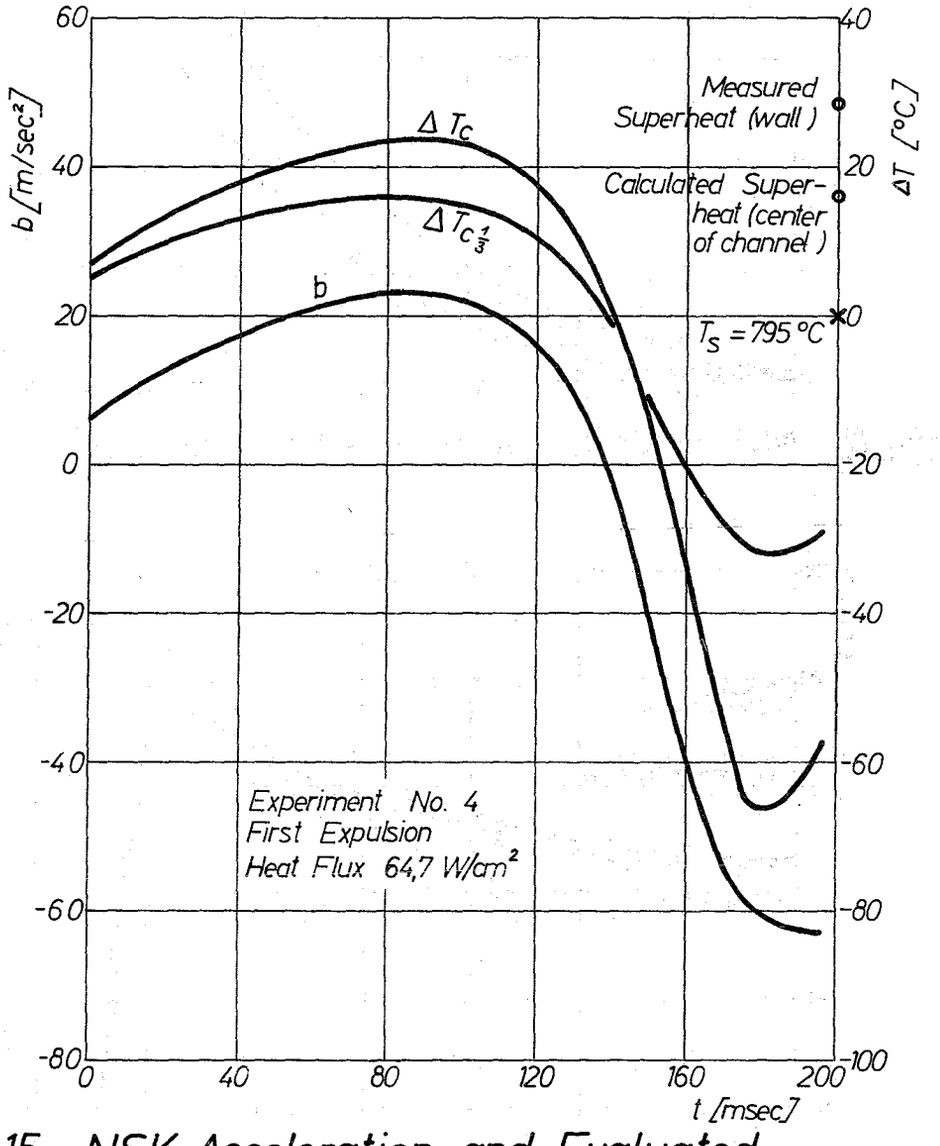

Fig.15 NSK Acceleration and Evaluated Driving Superheat vs Time During First Expulsion

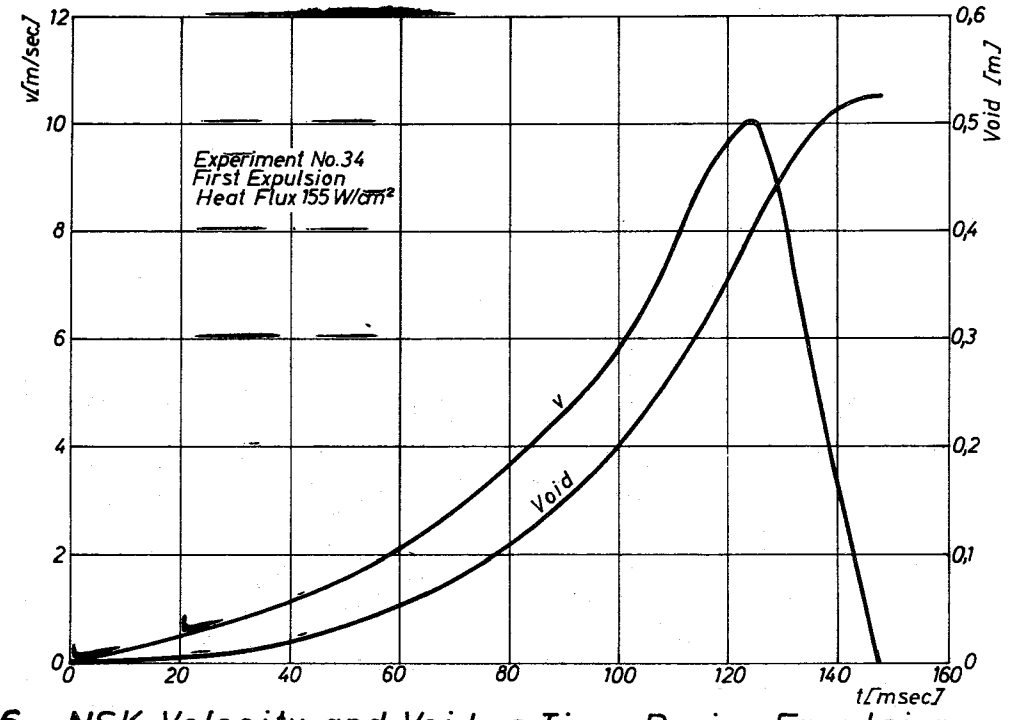

Fig. 16 NSK Velocity and Void vs Time During Expulsion

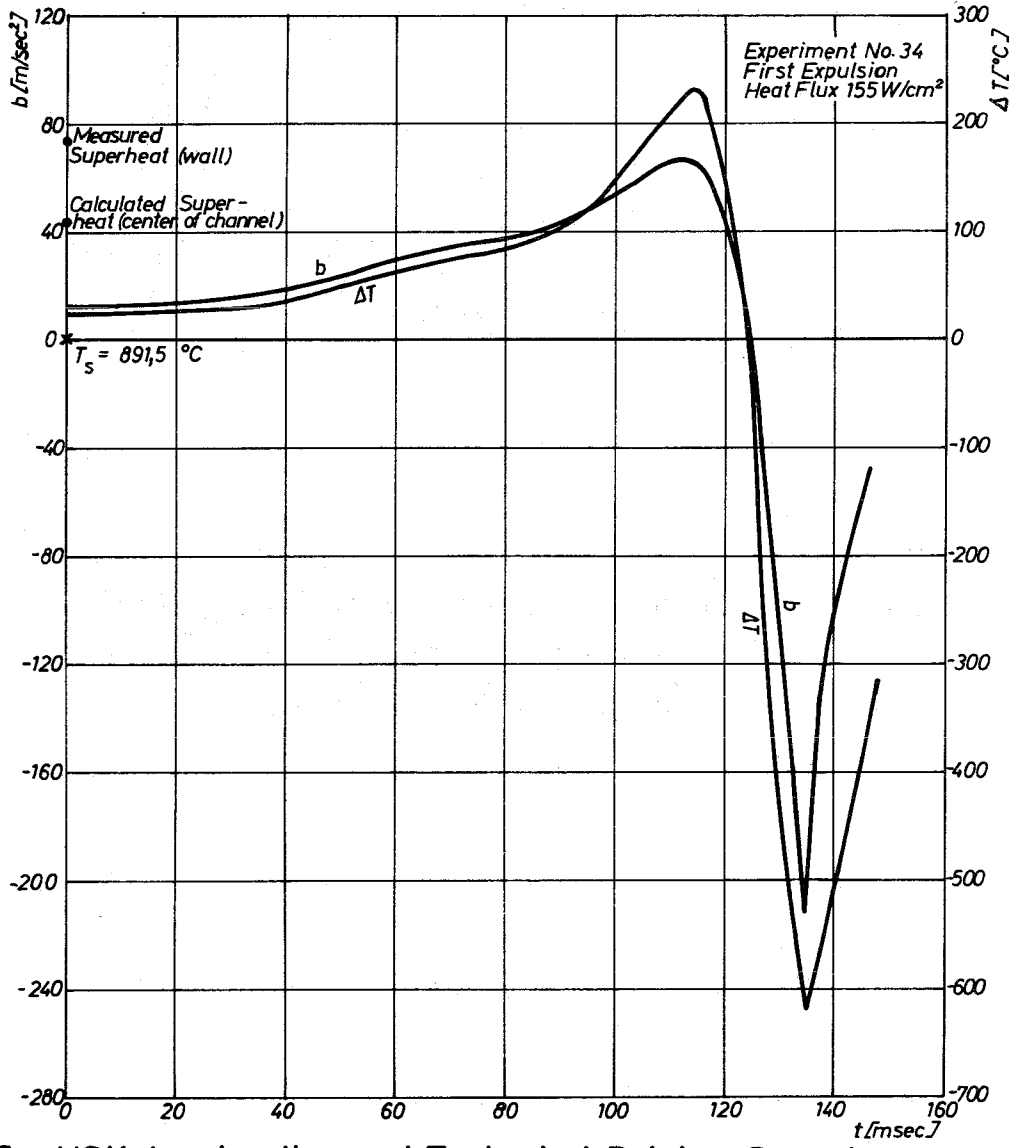

Fig. 17 NSK Acceleration and Evaluated Driving Superheat vs Time During First Expulsion

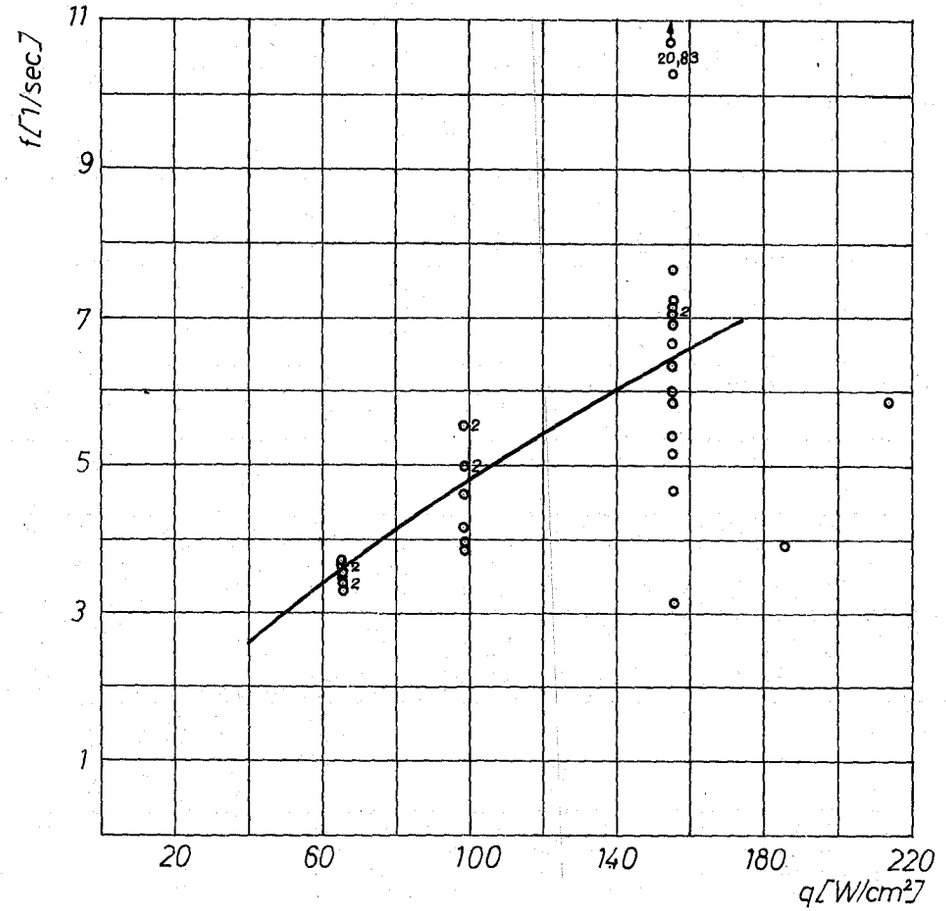

Fig.18 NSK Expulsion Frequency vs Heat Flux

No.	Pressure peaks [at]					
	1. reentry channel			x reentry or condensation(K)		
	2	4	5	2	4	5
4		0,5		6,75$_K$	0,625$_K$	1,0$_K$
5		16,5	16,5	12,0$_K$	16,5$_1$	16,5$_1$
6		7,4	3,9		8,7$_4$	0,4$_4$
7		10,2	16,0		10,2$_1$	16,0$_1$
8		-0,6			16,5$_2$	16,5$_2$
9		2,0	0,4	11,0$_K$	2,0$_K$	2,0$_K$
10		10,0	23,5		28,5$_2$	22,5$_2$
11		24,5	22,0		25,5$_3$	1,5$_3$
12		11,0	0,5	3,0	11,0$_2$	0,5$_2$
13		24,5	22,5		24,5$_1$	22,5$_1$
14		25,0	20,0		25,0	20,0$_1$
15		16,0	20,0		25,0$_2$	1,5$_2$
16		27,0	17,0		27,0$_1$	17,0$_1$
17		26,5	20,5	8,5$_K$	35,0$_K$	5,0$_K$
18					26,0$_2$	1,5$_2$
19				17,5$_K$	35,0$_K$	36,0$_K$
20	4	35,0	35,0	11,0$_K$	35,0$_K$	36,0$_K$
21		8,0		4,0$_2$	12,5$_2$	17,0$_2$
22				16,0	2,75	3,5$_7$
23		12,5	10,0		24,5	15,0$_2$
24		16,5	1,0		23,0	21,0$_2$
25						

No.	Pressure peaks [at]					
	1. reentry channel			x reentry or condensation(K)		
	2	4	5	2	4	5
26		5,0	0,5	31,4	35,0	35,0$_K$
27		3,5	0,25	4,5	17,5	13,5$_K$
28				22,0	3,0	3,0$_K$
29		0,75			20,0$_3$	
30		27,0	21,0	28,0	5,0	6,0$_K$
31		25,5			25,5$_{1-2}$	
32		14,5	15,0		25,0	27,5$_2$
33		4,5	11,0		22,5	25,0$_{2-3}$
34		7,0			20,0	17,5$_{1-2}$
35		26,0	20,0		26,0	~20,0$_{1-2}$
36		4,5	6,5	7,0$_K$	1,7$_K$	2,2$_K$
37	1,5	2,0	2,0	2,5$_K$	3,3$_K$	2,2$_K$
38		0,5	1,2	35,5	11,0	10,0$_K$
39		25,0	21,0	6,5	36,5	6,5$_K$
40		16,5		14,0	6,0	6,0$_0$
41		3,8		36,5	5,0	8,5$_K$
42	2,0		2,5	4,25	14,5	4,75$_K$
43						
44		24,0	~1,0	8,5	36,4	~36,4$_{2-3}$
45						
46				68,7	10,0	15,0$_K$
47		10,0	0,25	4,5	25,0	5,5$_K$

Table 19 NSK Maximum Pressure Peaks (Reentry)